JOURNAL OF MATERIALS SCIENCE 28 (1993) 161–169

Fine structure of defects in polyethylene used for power cable insulation observed by fluorescence microscopy

E. MOREAU, A. BOUDET
CEMES-LOE, CNRS, 29 rue Jeanne Marvig, BP 4347, 31055 Toulouse cedex, France

C. MAYOUX, C. LAURENT
Laboratoire de Génie Electrique, Université Paul Sabatier, bât. 3R1B3, 118 route de Narbonne, 31062 Toulouse cedex, France

M. WRIGHT
Laboratoire de Pharmacologie et de Toxicologie Fondamentales, 205 route de Narbonne, 31400 Toulouse, France

The growth of defects called watertrees in cross-linked polyethylene power-insulated cables is poorly understood. We characterized the watertree structure on artificially aged samples. The resolution of the observations was improved by contrasting watertrees with rhodamine, a fluorescent probe and using epifluorescence microscopy. Both video-enhanced microscopy and confocal laser scanning microscopy provided evidence that watertrees are constituted of continuous microchannels. Their diameter is irregular and ranges between 0.6 and 0.2 μm, and maybe less. They form a complex three-dimensional array that is accurately depicted.

1. Introduction

Power cables for underground service are made of an inner conductor, either aluminium or copper, jacketed by an insulating material. Polymers for insulation were introduced in the fifties to replace oiled paper, because they were expected to have a higher longevity together with a lower price [1]. Many different polymers usually extruded on to the conductor are used: low-density polyethylene, cross-linked polyethylene (XLPE), butyl rubber, ethylene–propylene copolymer, or ethylene–propylene–dien terpolymer. However, it was recognized in 1968 that after some years of use, cable failure occurred in the buried cables, evinced by the decrease of their resistance to alternative breakdown voltage [2]. Under the conjugated effects of the electric field and moisture, new figures, named watertrees, appeared inside the polymer. Watertrees are diffuse structures whose overall shape resembles a bush or a fan. Two types of watertrees were recognized: the "bow-tie trees" and the "vented trees", according to where these trees start growing. Bow-tie trees are initiated in the bulk of the insulating polymer and vented trees grow from the insulation surfaces. Their main axis lies along the radius of the cable. Then it was established that there was a correlation between the presence of watertrees and cable failure [3–5]. The presence of impurities like molecules of water and soluble ions scattered throughout the polyethylene may be a limiting factor for cable life. One of the main objectives in cable development is to increase the working electric stress. Reducing harmful defects in the insulation is thus a very important goal. Polymer-insulated power cables were initially in the voltage range 6–66 kV, but power cables with voltages 230, 345 and 400 kV are now under development.

Even if watertrees are generally accepted as the major cause of failure of polyethylene-insulated cables, the mechanism of watertreeing is not agreed upon. A survey of the literature on the formation of watertrees in solid dielectrics was presented in 1976 by Eichhorn [6]. More recently, Stennis and Kreuger reviewed watertree growth in polyethylene cables [7]. After the occurrence of a breakdown, small carbonized structures, named electric trees, can be seen. Clear pictures were published by several authors [1, 8–10] showing electrical trees grown from the branches of a watertree. However, it always remains difficult to characterize the exact relationships between the development of an electrical tree and the existence of the watertrees. As watertrees can act as an initiation site for electrical trees, it is necessary to know the detailed features of watertrees.

Watertrees have been studied in specimens extracted from real defective field-aged cables as well as from experimentally aged material obtained in the laboratory. Because field-aged cables are rarely available, most investigations have been performed on samples aged in the laboratory. On such specimens, it is easy to vary and control different parameters concerning the original polyethylene and the conditions of ageing. Recently, we showed that this simulation was valid because watertrees observed in aged cables and in samples aged in the laboratory were similar at the microstructural level [11].

0022–2461

Watertrees have been observed by light microscopy (LM) [9, 10, 12], scanning electron microscopy (SEM) [8, 13–15], transmission electron microscopy (TEM) [16–18], and autofluorescence microscopy [19]. Most authors, using LM [9, 10, 12] or SEM [13–15], assumed that watertrees are made of a distribution of small unconnected cavities of variable sizes, ranging from 1 to several micrometres. In contrast to this model, others observed hollow microchannels in SEM [8], or suggested from TEM observations, that microchannels could result from the coalescence of cavities as small as 0.1 μm diameter, thus interconnecting larger cavities [8, 16–18].

The difficulties of observing the details of the watertree structure explain why the investigators have proposed two different models. Both in scanning and transmission electron microscopy, in cross-sections, it is difficult to differentiate a spherical cavity from a cylindrical channel. The surface of the sections can also be strongly disturbed either by freeze fracture (SEM) or by sectioning (TEM). Moreover, it has been proven that the subsequent treatments with etchants and stains (permanganic, nitric and chromic acids, osmium tetroxide, carbon tetrachloride) which are applied to these sections, created many artefacts [14]. Observation by light microscopy, although very useful, is generally limited by the low natural contrast of the watertrees. Contrast enhancement is generally based upon the staining of the polymer cavities with methylene blue. However, this method did not allow one to distinguish very small cavities against the background due to light scattering.

We used epifluorescence light microscopy after staining of watertrees with a fluorescent dye. This method has been largely used in microscopical biological studies, where the fluorescent dye is generally covalently linked to a drug or an immunological probe. Although this method could not allow the separation of two fluorescent points less than 0.22 μm apart with the best objectives available [20], it offers the possibility to detect very small objects far below the resolution of the microscope if they are separated by more than 0.22 μm. Thus, observation of isolated objects ranging from 30–5 nm diameter is routinely achieved [20, 21]. Epifluorescence microscopy is currently operated with a standard video-enhanced light microscope, i.e. a microscope equipped with a video camera and a computer used to digitize, record and process the images. As the out-of-focus fluorescence impairs the contrast of the images, we also used a confocal laser scanning microscope in epifluorescence mode [22]. Schematically, the laser source is focused inside the specimen so that the fluorescence is emitted by a punctual source. Then fluorescence of this source is preferentially collected on a photomultiplier, recorded in a computer, and the three-dimensional image is reconstructed by scanning the specimen. This method improves the contrast and allows the superposition of optical sections of 0.5 μm.

The images obtained on watertrees by these two techniques are presented here for the first time.

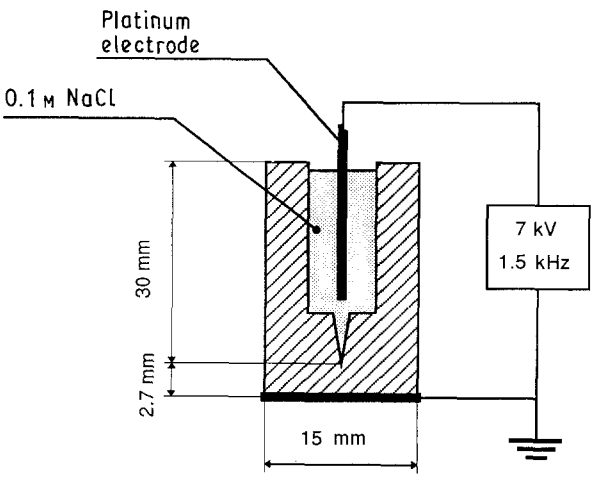

Figure 1 Diagram of the ageing bench for the needle test.

2. Experimental procedure

2.1. Specimens

The material studied was a cross-linked polyethylene (XLPE) in which an antioxidant (Irganox 1081) was added at 3000 p.p.m. Cross-linking was obtained chemically by addition of 2% dicumyl peroxide. After polymerization, the samples were heated to 70 °C in vacuum over 10 days in order to evacuate the residual by-products of the cross-linking reactions and to release residual strains. Samples were moulded according to the shape and measurements depicted in Fig. 1. Then they were aged artificially by the usual needle test [23]. A needle was inserted in the block before solidification and then withdrawn. The remaining hollow cone was filled with an aqueous solution of 0.1 M NaCl in order to form a liquid electrode (waterneedle). Then, an alternative voltage of 7 kV at 1.5 kHz was applied for more than 20 h at room temperature. Watertrees grew at or close to the tip of the waterneedle under optical control.

2.2. Microscopic observations

Before sectioning, the specimens were dried at 60 °C for 30 min to remove water which could be present in the watertrees because residual water could fracture the material during the subsequent freezing procedure. Then, 10 μm thick sections were obtained from the specimen by cryo-ultramicrotomy performed at − 100 °C, so that the specimen was rigid enough to be easily sectioned. The sections were cut both along the axis of the needle and in cross-sections.

In some specimens, contrast was enhanced by filling watertrees with water or by staining them with methylene blue according to the usual procedure [24, 25]. Alternatively, contrast was enhanced with rhodamine, a fluorescent probe which can be observed in epifluorescence microscopy and confocal laser scanning microscopy. Thin sections were immersed in a 70 μg/ml solution of rhodamine at 60 °C, for 4 h or more and then washed in water before observations.

Sections were observed with a Zeiss Axiophot microscope in bright-field and epifluorescence modes (excitation filter BP 546 nm/12; emission filter

LP > 590 nm). The images were recorded with a Nocticon camera (Lhesa), digitized and submitted to an image-enhancing treatment (Quantel : image averaging, histogram and stretch functions). Some sections were observed with a confocal laser scanning microscope (Zeiss CLSM) in order to obtain three-dimensional images of the specimen up to 50 µm thick. Entire watertrees could be recorded because the depth of the watertrees was estimated to be about 15–25 µm.

3. Results

3.1. General aspects and shape of the watertrees

When contrasted by water and observed in bright-field microscopy (Fig. 2), the specimen exhibited watertrees with the usual figures already described [9]. Trees grew from the tip of the needle and from the sides. Their shapes were variable, either fan-like or bush-like. Their boundaries were very well delimited, but no internal details of the structure of the tree were visible, with the exception of contrasting lines radiating from the interface, in which it was impossible to distinguish any internal structure. More details were observed in contrasting watertrees with methylene blue (Fig. 3). The contrast was better and it was apparent that watertrees were made of bundles possessing an apparent filamentous nature and oriented radially. These bundles accounted for the previously observed "radiating lines". However, it was not possible to determine the internal structure of these filaments.

When watertrees were contrasted with rhodamine and observed by epifluorescence videomicroscopy (Fig. 4), the areas containing rhodamine showed a clear red fluorescence. A faint background of fluorescence was observed, showing that the fluorescence inside the polyethylene was very low compared to the bright fluorescence of the rhodamine filling the watertrees. The relative background fluorescence was much lower than the background observed when watertrees were filled with water (Fig. 2) or dyed with methylene blue (Fig. 3). The general outline of the watertree was preserved and the same characteristic features of the bundles could be observed.

When examined at different places in the same sample, watertrees exhibited different morphologies (Figs 4–6, the locations of these figures are shown in Fig. 7). Some watertrees were found at the tip of the needle and some were found along its side. At the tip (Fig. 4), watertrees exhibit a bushy appearence. In contrast, on the sides (Figs 5 and 6) they were of narrow fan shapes and, in many samples, they were curved towards the rear of the needle. Despite these differences in their overall morphologies, they all consisted of several oriented bundles with a complex substructure which will be described below. The lengths of the bundles remained approximately the same throughout the watertrees. Between the bundles, areas without fluorescence were observed. They showed no visible structure (Fig. 6; areas marked X). Watertrees seemed to possess a "foot" at the interface of the needle located on narrow spots dispersed inhomogeneously along the edge of the needle print. Sometimes part of the watertrees close to the foot was very narrow and became wider only at some distance from the foot (Fig. 4).

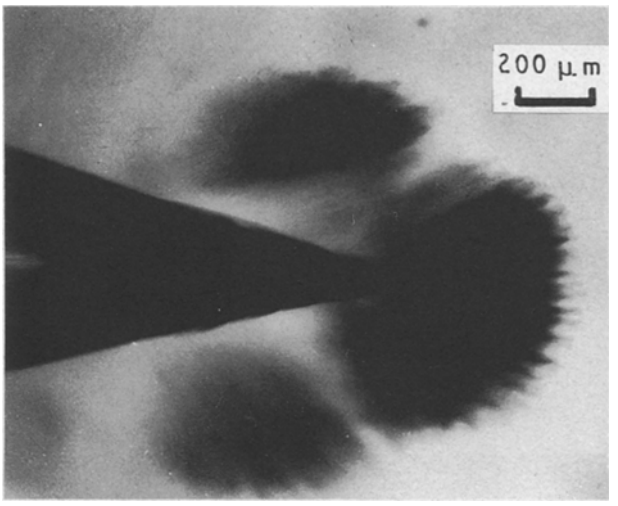

Figure 2 Watertrees grown from a waterneedle. Radiating lines are visible on the edge of the needle. Watertrees have been contrasted with water and observed in light bright-field microscopy.

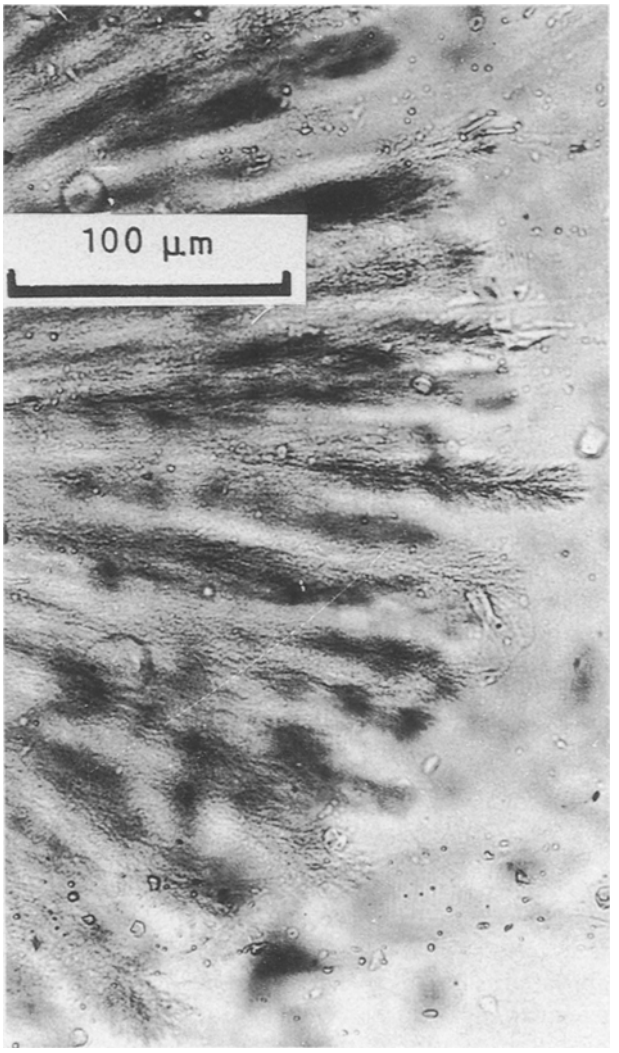

Figure 3 Part of a watertree showing a fan of bundles. Watertrees have been contrasted with methylene blue and observed in light bright-field microscopy.

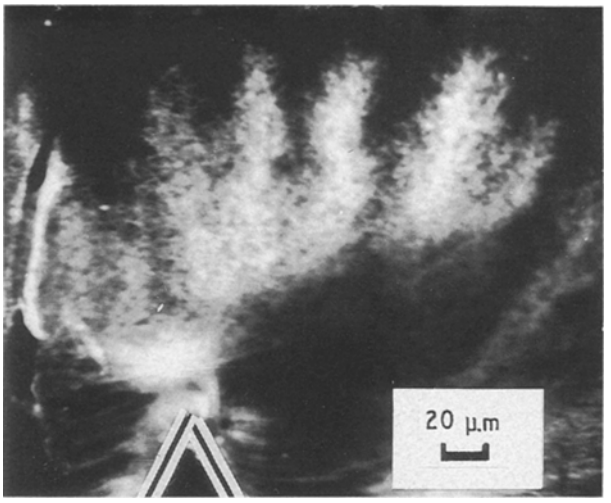

Figure 4 A watertree grown at the tip of the needle, stained with rhodamine and observed by epifluorescence microscopy.

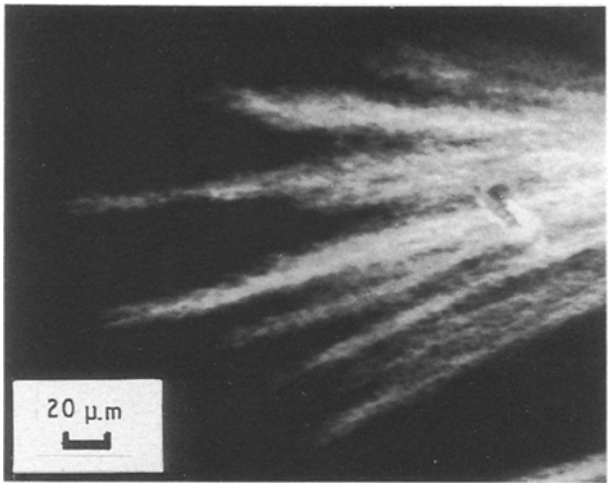

Figure 5 A watertree grown on the side of the needle, stained with rhodamine and observed by epifluorescence microscopy.

3.2. Description of the channels

Increasing the magnification revealed that the bundles were constituted of numerous small fluorescent spots. Fig. 8 is a larger scale view taken at the tip of a bundle shown in Fig. 5. Observation of a single picture in a focal plane could suggest that these bundles are formed of adjacent cavities filled with rhodamine. However, when the focus of the objective lens was shifted towards other focal planes, other spots came into view and drew continuous tracks deep in the specimen, connecting the spots which initially appeared isolated (Fig. 9a and b, spots D–D′, F–F′). A few other spots could not be connected by changing the focus. The apparent disconnection of the spots in a single focal plane is due to the small depth of field of the microscope which detects only optical cross-sections inside the sample (Fig. 10). Therefore, watertrees appeared as fine microchannels spreading along a very irregular array in three dimensions. Although the overall orientation of the bundle was clearly defined, the local orientation of the microchannels seemed to be random and independent of the definite orientation of the bundle that they contributed to form. They went

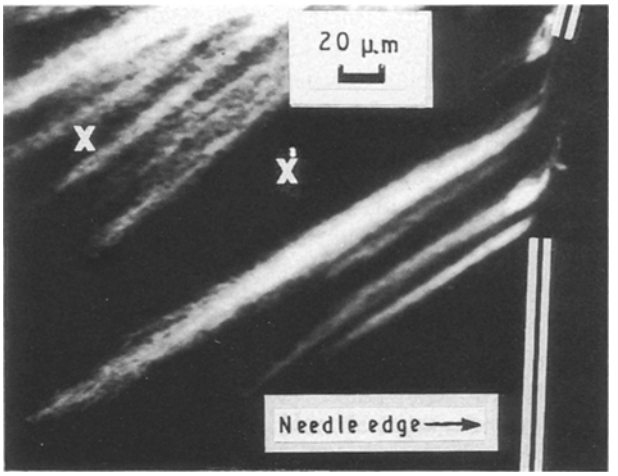

Figure 6 Watertrees with well-separated feet on the side of the needle, stained with rhodamine and observed by epifluorescence microscopy. The areas marked X are examples of areas without fluorescence.

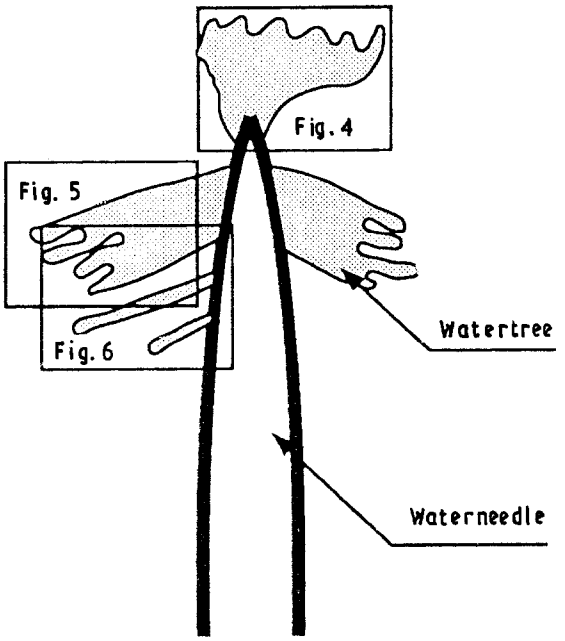

Figure 7 Diagram showing the relative locations of the previous figures. The watertrees are represented by the shaded areas.

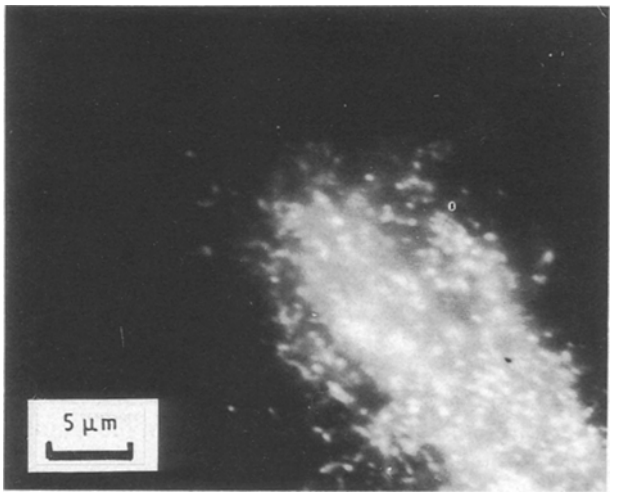

Figure 8 Detail of the tip of a bundle. Numerous rhodamine fluorescent spots are visible.

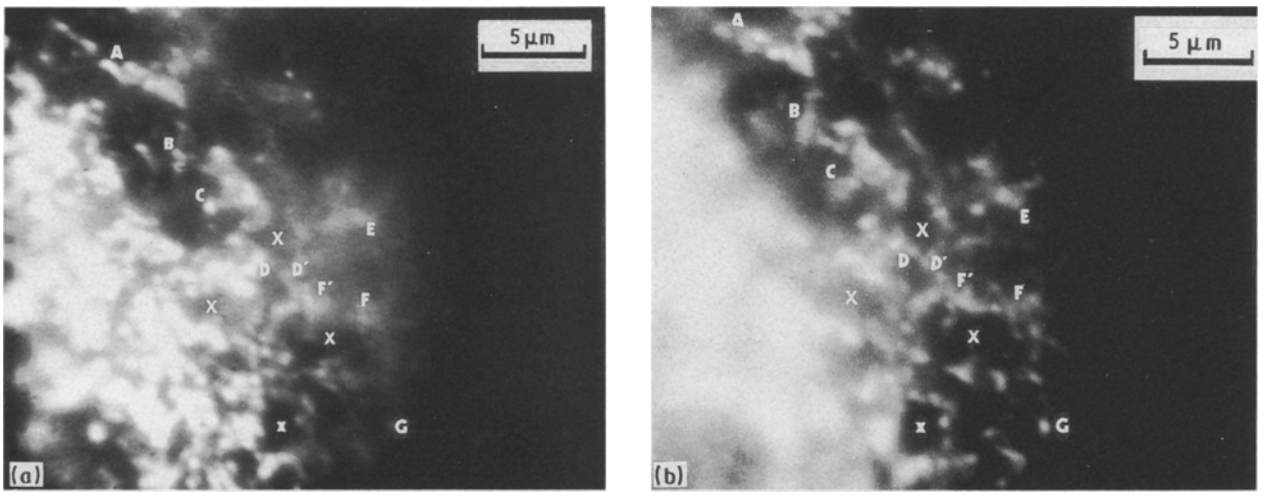

Figure 9 Detail of a part of a bundle at two successive focal planes (a and b). The capital letters are markers to locate the same place of the sample in (a) and (b). See connections between D and D', F and F'. More or less circular areas without fluorescence delimited by rings of microchannels are marked X.

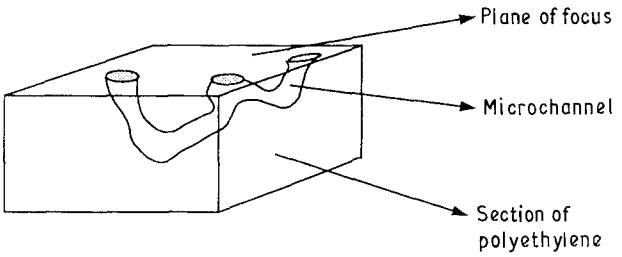

Figure 10 Diagram showing the appearance of a microchannel when crossed by a low depth-of-focus plane.

up and down, left and right and were very entangled. Inside the bundles, the local density of microchannels was also heterogeneous. Some areas were densely crossed by channels and others exhibited no fluorescent channels or spots. These small areas usually showed a more or less circular shape about 2 µm diameter, and were delimited by microchannels that seemed to be displayed in rings when viewed in the two-dimensional image resulting from the projection of a three-dimensional structure (Fig. 9, areas marked X).

This three-dimensional structure of the channels has been confirmed and its description improved in recording the different images of each focal plane by confocal laser scanning microscopy (Fig. 11). The images of each optical section were then processed in order to obtain a three-dimensional image which could be provided as a stereo pair (Fig. 12). The recordings of the different optical sections showed that the thickness of the watertrees did not exceed 20–25 µm. It was recognized that the microchannels surrounding areas without fluorescence (Fig. 9) were not rings, but open structures more resembling helices. However, in these first observations, there was no opportunity to verify whether these microchannels were connected together into an array offering continuous paths from the root to the apices of the bundles. What could be seen were parts of an array of entangled and connected channels. Mixed with them, some segments of channels were visible, and, sometimes, small elongated isolated spots.

In Fig. 13, an enlarged image shows a microchannel where we could observe the detailed shape. Within the limits due to the resolution as discussed below, it was apparent that the diameter of the channel was irregular. Rough measurements on the micrograph provided values varying from 0.2–0.6 µm.

4. Discussion

4.1. Epifluorescence microscopy

No conclusion concerning the structure of microchannels can be drawn without discussing the limitations of microscopy observations (resolution, depth of field) and how the rhodamine fluorescence can provide reliable images of the real structure of watertrees: (1) does rhodamine fill or mark the tracks of the watertree without modifying it?; (2) how the resolution and the depth of field of the videomicroscope and of the scanning confocal microscope limit our knowledge of this structure; (3) does rhodamine stain the whole watertree?

Most of our previous knowledge about the structure of watertrees was obtained from images contrasted either by water immersion or by methylene blue. From our images at the same scale, we can conclude that the images of the watertrees obtained in epifluorescence using rhodamine as a fluorochrome are similar and show the same general aspects. However, epifluorescence both in videomicroscopy and confocal microscopy gave images with a higher contrast, due to the decrease of the background, so that higher magnifications could be achieved. This background is due to the autofluorescence of the polyethylene out of the watertree, and/or to the fluorescence of rhodamine that diffused in the undamaged polyethylene. Relative measurements of the brightness on unprocessed pictures, from 0–100 in arbitrary units, showed that the brightness of the watertrees varied from 24–100 while the background (black in our photographs) remained

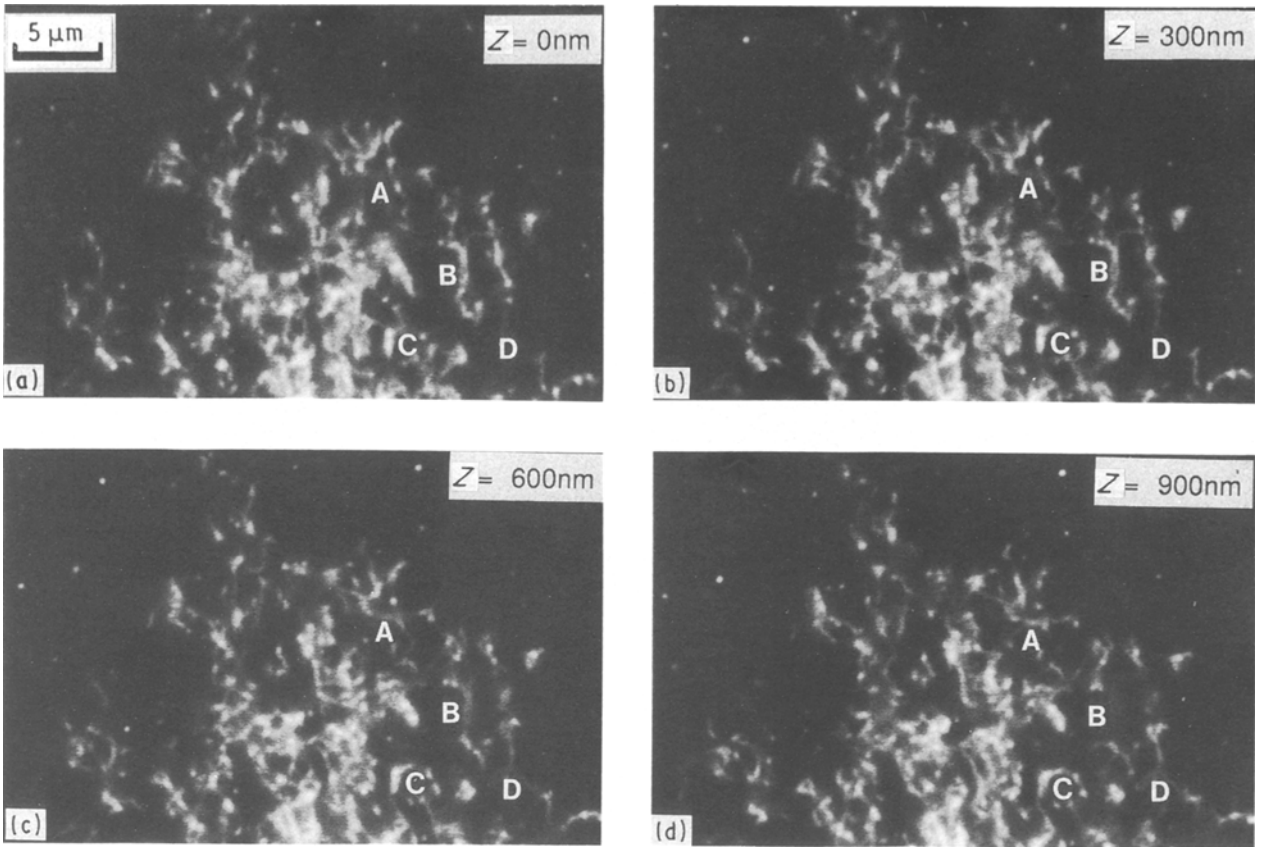

Figure 11 A series of four successive optical sections obtained in confocal laser scanning microscopy. Sections are separated by a 300 nm depth. The capital letters are markers to locate the same place of the sample on the different sections. One can find many examples of isolated points that are connected on another level (A, B, C, D), or can be seen at several levels, thus revealing a vertical channel (C).

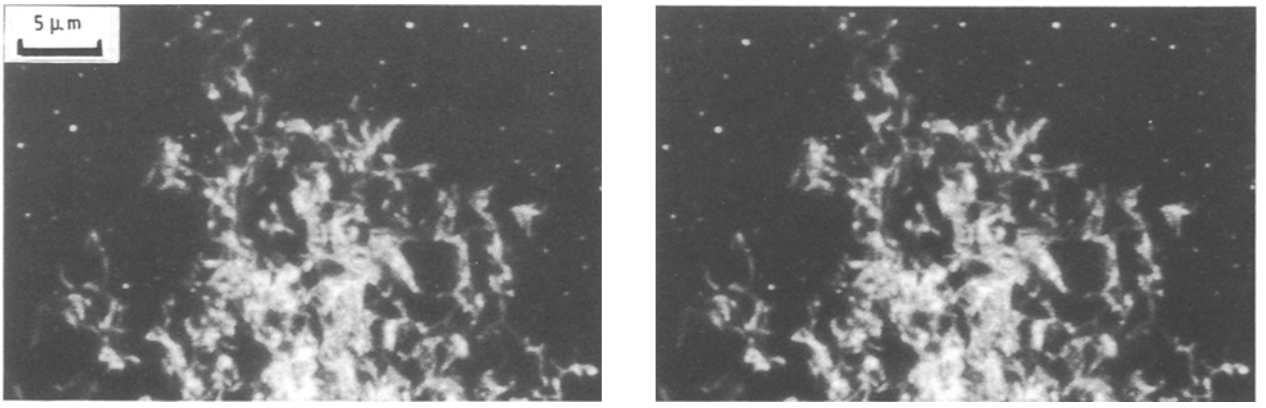

Figure 12 Stereo pair showing the microchannels in three dimensions. Reconstruction obtained in confocal laser scanning microscopy from six 300 nm thick optical sections including the four sections displayed in Fig. 11.

in a 0–14 range. Furthermore, epifluorescence observations using confocal microscopy provided valuable information in three dimensions that has never been obtained with water or methylene blue contrasts. Some physical or chemical effects of rhodamine, as well as water and methylene blue, on polyethylene cannot be excluded at the molecular level, but it is very unlikely that rhodamine could induce perturbations at the supramolecular level observed (20 nm or higher), i.e. in the range of structures that could be detected by epifluorescence microscopy.

4.2. Diameter of microchannels

The maximum resolution which could be reached with the best oil-immersed objective (×63, numerical aperture 1.4) was about 220 nm. Schematically, this implies that two points separated by a distance less than 220 nm could not be distinguished from one another. However, isolated smaller particles up to 5 nm diameter could be detected [20, 21]. Due to the diffraction of light, on the other hand, their apparent size is far larger, so that an uncertainty of about 100 nm in the measurements cannot be avoided. All measurements made at the level of the maximal resolution of the microscope allow estimation of the upper limit of the apparent diameter, but not the real diameter. Therefore, the smaller apparent diameter value (200 nm) of the channels is only a rough estimation, as

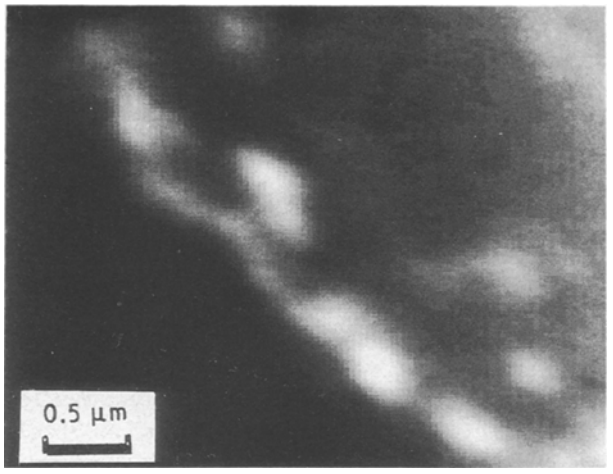

Figure 13 High magnification image of a part of a microchannel, stained with rhodamine and observed by epifluorescence microscopy.

it could be much smaller. The presence of continuous channels, as discussed below, does not imply that their diameter is constant. In fact, our observations demonstrated that the sections of channels are variable, even if it is not possible to determine their actual size. More precise measurements of microchannel diameters could only be obtained by electron microscopy.

4.3. Cavities or channels?

We have shown that watertrees were constituted by segments of microchannels building an array or parts of arrays, with a few isolated spots accompanying them. Of course this holds only within the limits of resolution. First, we cannot distinguish two points separated by a distance smaller than 220 nm in a focal plane, thus we cannot differentiate a continuous path from a sequence of small cavities closer than 220 nm. Second, we cannot distinguish two cavities superimposed and located in two adjacent focal planes from a continuous vertical channel. Observations both in videomicroscopy or in confocal scanning microscopy are limited by the large depth of field of the objective lenses varying from 0.66, 0.27, and 0.32 µm for the ×40 (NA:0.90), ×63 (NA:1.40), and ×100 (NA:1.30) objectives, respectively. However, it is unlikely that several focal planes could repeatedly display a channel appearence with superimposed cavities.

Despite this limitation, we can compare our results with the model based on electron microscopy observations [8, 16–18]. It has been claimed that watertrees were constituted of microvoids of 10–100 nm diameter. These conclusions have to be considered very carefully. In electron microscopy, the specimen is sectioned into about 100 nm thick thin films, thus the channels could have been cut and could appear as isolated cavities exactly in the same way as in the optical sections (Fig. 10). But the main difficulty in electron microscopy is the impossibility to distinguish between holes constituting the watertree, holes present in the polymer before ageing out of the watertree, and holes resulting from a harmful preparation procedure. Although electron microscopic studies have not been intended to evaluate the absolute distances between cavities, estimations from the published pictures [16, 18] suggest distances above 200 nm and most often above 500 nm, values that could have been resolved easily in epifluorescence microscopy. From our observations (see especially Figs 12 and 13), it is obvious that microchannels are mainly present in the watertree area. Figures resembling sequences of spots with discontinuities are visible, but changes in the focus and fine inspection of the photographs most often reveal a faint connection between them. This is not always the case, as some channels can be interrupted and a few of them appear only as small elongated cavities. As these observations have been performed on well-developed watertrees, it would be necessary to study the newly formed watertrees to determine if these channels are already present at the beginning or if vacancies are formed first, becoming closer and closer and eventually coalescing.

Our observations support the view that well-developed watertrees are constituted by microchannels rather than sequences of isolated cavities. However, these microchannels may be segmented, and it is not proved that these channels build a continuous path from the root to the tip of the branches.

4.4. Nucleation of watertrees

The feet of watertrees, located at the surface of the waterneedle print, would logically correspond to their nucleation point. The location of these feet on precise areas must be due to some special local conditions existing in these spots, favouring the initiation of destructuring. The nature of these conditions could be topological, chemical, mechanical, structural or electrical. (1) The interface between the polymer and the needle could possess some corrugations or bump. (2) Chemical impurities could be located on it. (3) Residual stresses due to the moulding of the polymer could be stronger in some places. (4) Particular arrangements of the crystalline lamellae or the amorphous part could offer areas of preferential destructuration. (5) Finally, the electric field could be heterogeneous and could reach critical values at certain spots. These conditions are not independent. For instance, the local structure could result from residual stresses, and the local electric field could be determined by chemical, topological and structural peculiarities. But up to now, we have found no indications allowing us to assess the relative role of each of these parameters.

4.5. Shapes and orientations

Why are the shapes of the different parts of the watertrees so different, especially between the tip and the sides of the waterneedle? Different factors could influence the local expansion and growth of the watertree, in the same way as they influence nucleation spots: the shape of the needle, heterogeneous distribution of additives like antioxidant or water, the moulding process, or microstructure disturbing the local electric field. The initial form of the granules of polyethylene with subsequent heating and pressure, the

differences of temperature between the bulk and the surface of the mould during cooling and the shape of the needle would create heterogeneities and residual stresses. Moreover, paths with a different mechanical resistance inside the polyethylene could be present close to the tip of the needle and to the side.

Because watertrees grow from the tip of the needle which is an electrode, and the bundles diverge from this electrode, it could be expected that the orientation of these bundles follows the force lines of the theoretical electric field between the two electrodes (needle and plate, Fig. 1). However, it is obvious that there is no direct relationship between the growth of the bundles and these expected force lines. A first explanation is that the real microscopic electric field is probably very different from the theoretical one, because of the heterogeneities present in the structure. Another likely possibility is that the path of the watertree could result from two main influences, the electric field and the mechanical resistance of the material, both contributing to chemical changes.

4.6. Entanglement of microchannels

The way the microchannels are displayed inside the bundles is very surprising. Although the bundles appear with a very well delimited outline and a definite orientation, they are constituted by erratic and entangled channels, which sometimes display a circular or a rather helicoidal path. It is very difficult to suggest a mechanism relating these two features. However, there is some indication that the microchannels could grow around the crystallites or their arrangements such as spherulites. This has already been proposed by Muccigrosso and Phillips [26], although Bamji *et al.* [14] demonstrated that the nodules visible in scanning electron microscopy were not spherulites and were due to the preparation of the specimen with etchants. Nevertheless, our preliminary observations in polarized light microscopy on low-density polyethylene seem to support a structure made of spherulites bounded by microchannels. However, the spherulites are not well formed in cross-linked polyethylene and it is not definite that they are the most common structure. Therefore, it is necessary to investigate this problem further on samples made of linear low-density polyethylene. Furthermore, the thickness of the specimen suitable to observe watertrees is too large to observe clearly the shapes of the spherulites.

5. Conclusion

Epifluorescence microscopy is a very suitable way to visualize watertrees inside aged polyethylene. It allowed us to reach a better resolution of the images of the inner structure of the tree, and at the same time, these images offered a good general view of the complex figure of the bundles. Although it is easier to observe watertrees by epifluorescence with a standard microscope, the use of a confocal laser scanning microscope gave images devoided of out-of-focus fluorescence and allowed the three-dimensional reconstruction of the microchannels.

We were able to determine that watertrees start on well-defined spots at the surface of the waterneedle. The nature of these spots remains undetermined. Microchannels grow along erratic paths entangling with respect to one another in three dimensions, most likely according to the arrangement of crystalline and amorphous parts and to heterogeneous values of the electric field. Their diameter is variable but very small, more often less than 0.6 μm and sometimes less than 0.2 μm. Microchannels are connected to each other in more or less large arrays, but it was impossible to determine if there was a continuous path between them. Some channels are short and seem isolated. More or less elongated isolated cavities can also be found.

On the basis of our observations, we suggest that, at least for the well-developed watertrees present in our specimens and within the limit of the 0.2 μm resolution, microchannels are not formed by the juxtaposition of isolated cavities. In contrast, we showed that the so-called cavities are connected at different depths inside the polyethylene.

Acknowledgements

The confocal microscopy was performed by Mr Freiss and Mr Gonindard, in the laboratory of Dr Dussourd d'Hinterland and Mrs Pinel (Pierre Fabre Médicament) who are gratefully thanked. The authors are indebted to ATOCHEM and Cables Pirelli for their financial support.

References

1. R. D. NAYBOUR, *IEEE Elect. Insul. Mag.* **6** (5) (1990) 20.
2. J. H. LAWSON and W. VAHLSTROM, *IEEE Trans.* **PAS-92 T72502-3** (1973) 824.
3. T. MIYASHITA, *IEEE Trans.* **EI-6** (1971) 129.
4. T. TABATA, T. FUKADA and Z. IWATA, in "Proceedings of the IEEE Meeting and International Symposium on High Power Testing", Portland (1971), 71TP545-PWR, 1370.
5. W. VAHLSTROM Jr, *IEEE Trans.* **PAS-91 71C42-PWR** (1972) 1023.
6. R. M. EICHHORN, *IEEE Trans. Elect. Insul.* **EI-12** (1) (1976) 1.
7. E. F. STENNIS and F. H. KREUGER, *ibid.* **25** (5) (1990) 989.
8. W. KALKNER, V. MÜLLER, E. PESCHKE, H. J. HENKEL and R. VON OLSHAUSEN, in "Proceedings of the CIGRE International Conference on Large High Voltage Electric Systems", Paris 21-07 (1982) 12.
9. J. C. FILIPPINI, J.Y. KOO, Y. POGGI, C. LAURENT, C. MAYOUX and S. NOEL, in "Proceedings of the International Conference on Polymer Insulated Power Cables JICABLE" (1984) 87.
10. J. L. CHEN, P.C. FILIPPINI and Y. POGGI, in "Conference Recordings of the International Conference on Properties and Applications Dielectric of Materials", 85-CH2115-4, Xian, June 1985, p.366.
11. E. MOREAU, A. BOUDET, C. MAYOUX, C. LAURENT, in "Proceedings of the Third International Conference on Properties and Applications on Dielectric Materials" ICPADM, Tokyo, July 1991, p.232.
12. K. ABDOLALL, H. E. ORTON and M. W. REYNOLDS, "1985 Annual Report of the Conference on Electrical Insulators and Dielectric Phenomena", CEIDP.
13. H. ORTON, K. ABDOLALL, S. BAMJI, A. BULINSKI, J. DENSLEY and A. GARTON, in "1981 Annual Report of the Conference on Electrical Insulators and Dielectric Phenomena" CEIDP, p. 306.

14. S. BAMJI, A. BULINSKI, J. DENSLEY and A. GARTON, *IEEE Trans. Elec. Insul.* **EI-18** (1) (1983) 32.
15. S. BAMJI, A. BULINSKI, J. DENSLEY, A. GARTON and N. SHIMIZU, in "1984 Annual Report of the Conference on Electrical Insulators and Dielectric Phenomena", CEIDP, p. 141.
16. L. J. ROSE, V. ROSE and J. J. DE BELLET, in "Proceedings of the Second International Conference on Conductivity and Breakdown in Solid Dielectrics ICSD, Erlangen (1986) p. 237.
17. J. J. DE BELLET, G. MATEY, L. J. ROSE, V. ROSE, J. C. FILIPPINI, Y. POGGI and V. RAHARIMALALA, *IEEE Trans. Elec. Insul.* **EI-22** (2) (1987) 211.
18. L. J. ROSE, V. ROSE and J. J. DE BELLET, in "Proceedings of the Third International Conference on Polymer Insulated Power Cables JICABLE 87" (1987) p. 283.
19. R. ROSS, W. S. M. GEURTS, J. J. SMIT, J. H. VAN DER MAAS and E. T. G. LUTZ, in "Proceedings of the Third International Conference on Solid Dielectrics", CH 27268 (Trondheim, 1989) p. 512.
20. S. INOUE, "Videomicroscopy" (Plenum Press, New York, 1986).
21. B. J. SCHNAPP, R. D. VALE, M. P. SCEETZ and T. S. REESE, *Cell* **40** (1985) 455.
22. T. WILSON and C. J. R. SHEPPARD, "Theory and Practice of Scanning Optical Microscopy" (Academic Press, New York, 1984).
23. M. SAURE and W. KALKNER, in "Proceedings of the CIGRE Symposium S05-87", Vienna, 1987 p. 15/21-03.
24. A. C. ASHCRAFT and R. M. EICHHORN, *IEEE Trans. Elec. Insul.* **EI-13** (3) (1978) 198.
25. P. B. LARSEN, *Electra* **86** (1983) 53.
26. J. MUCCIGROSSO and P. J. PHILLIPS, *IEEE Trans. Electr. Insul.* **EI-13** (3) (1978) 172.

Received 27 November 1991
and accepted 24 March 1992